Original Article

Tumor Biology

Tumor Biology
October 2017: 1–18

DOI: 10.1177/1010428317695933
journals.sagepub.com/home/tub
SAGE

Antitumor effectiveness and mechanism of action of Ru(II)/amino acid/diphosphine complexes in the peritoneal carcinomatosis progression

Francyelli Mello-Andrade[1], Wanderson Lucas da Costa[1], Wanessa Carvalho Pires[1], Flávia de Castro Pereira[1], Clever Gomes Cardoso[2], Ruy de Souza Lino-Junior[3], Vicente Raul Chavarria Irusta[4], Cristiene Costa Carneiro[5], Paulo Roberto de Melo-Reis[6], Carlos Henrique Castro[7], Marcio Aurélio Pinheiro Almeida[8], Alzir Azevedo Batista[9] and Elisângela de Paula Silveira-Lacerda[1]

Abstract

Peritoneal carcinomatosis is considered as a potentially lethal clinical condition, and the therapeutic options are limited. The antitumor effectiveness of the [Ru(L-Met)(bipy)(dppb)]PF_6 **(1)** and the [Ru(L-Trp)(bipy)(dppb)]PF_6 **(2)** complexes were evaluated in the peritoneal carcinomatosis model, Ehrlich ascites carcinoma–bearing Swiss mice. This is the first study that evaluated the effect of Ru(II)/amino acid complexes for antitumor activity in vivo. Complexes **1** and **2** (2 and 6 mg kg^{-1}) showed tumor growth inhibition ranging from moderate to high. The mean survival time of animal groups treated with complexes **1** and **2** was higher than in the negative and vehicle control groups. The induction of Ehrlich ascites carcinoma in mice led to alterations in hematological and biochemical parameters, and not the treatment with complexes **1** and **2**. The treatment of Ehrlich ascites carcinoma–bearing mice with complexes **1** and **2** increased the number of Annexin V positive cells and cleaved caspase-3 levels and induced changes in the cell morphology and in the cell cycle phases by induction of sub-G1 and G0/G1 cell cycle arrest. In addition, these complexes reduce angiogenesis induced by Ehrlich ascites carcinoma cells in chick embryo chorioallantoic membrane model. The treatment with the LAT1 inhibitor decreased the sensitivity of the Ehrlich ascites carcinoma cells to complexes **1** and **2** in vitro—which suggests that the LAT1 could be related to the mechanism of action of amino acid/ruthenium(II) complexes, consequently decreasing the glucose uptake. Therefore, these complexes could be used to reduce tumor growth and increase mean survival time with less toxicity than cisplatin. Besides, these complexes induce apoptosis by combination of different mechanism of action.

[1]Laboratório de Genética Molecular e Citogenética, Departamento de Genética, Instituto de Ciências Biológicas, Universidade Federal de Goiás, Goiânia, Brazil
[2]Departamento de Morfologia, Instituto de Ciências Biológicas, Universidade Federal de Goiás, Goiânia, Brazil
[3]Laboratório de Patologia Geral, Departamento de Microbiologia, Imunologia, Parasitologia e Patologia, Instituto de Patologia Tropical e Saúde Pública, Universidade Federal de Goiás, Goiânia, Brazil
[4]Laboratório de Patologia Clínica, Hospital Araújo Jorge, Goiânia, Brazil
[5]Laboratório de Radiobiologia de Microrganismos e Mutagênese, Instituto de Ciências Biológicas, Universidade Federal de Goiás, Goiânia, Brazil
[6]Laboratório de Estudos Experimentais em Biotecnologia, Departamento de Biomedicina, Pontifícia Universidade Católica de Goiás, Goiânia, Brazil
[7]Laboratório de Fisiologia Autonômica e Cardíaca, Departamento de Fisiologia e Farmacologia, Instituto de Ciências Biológicas, Universidade Federal de Goiás, Goiânia, Brazil
[8]Centro Tecnológico, Coordenação de Ciência e Tecnologia, Universidade Federal do Maranhão, São Luís, Brazil
[9]Departamento de Química, Universidade Federal de São Carlos, São Paulo, Brazil

Corresponding authors:
Elisângela de Paula Silveira-Lacerda, Laboratório de Genética Molecular e Citogenética, Departamento de Genética, Instituto de Ciências Biológicas, Universidade Federal de Goiás, Goiânia, Goiás 74690-900, Brazil.
Email: elacerda@ufg.br

Alzir Azevedo Batista, Departamento de Química, Universidade Federal de São Carlos, São Paulo 13565-905, Brazil.
Email: daab@ufscar.br

Keywords
Ruthenium, peritoneal carcinomatosis, antitumor activity, angiogenesis, LAT1, apoptosis

Date received: 20 September 2016; accepted: 23 December 2016

Introduction

Peritoneal carcinomatosis is a locoregional cancer widespread within the peritoneal cavity and may occur as result of metastatic primary lesion from the stomach, ovary, intestine, colorectal, and, less commonly, lung and breast. It is considered potentially lethal clinical condition.[1–3] Usually, progression of the disease is associated with formation malignant ascites that causes abdominal pain and pressure, bloating, fatigue, nausea, and anorexia.[4,5]

The therapeutic options for peritoneal carcinomatosis are limited because complete surgical removal is not possible and systemic chemotherapy is not effective due to low concentration within the peritoneal cavity.[6] However, currently the treatment options have improved significantly. Intraperitoneal chemotherapy was introduced in treatments of peritoneal carcinomatosis to increase drug levels locally.[7]

Thus, metallodrugs are being developed to help overcome the limitations of the efficacy and safety of current cancer therapies.[8,9] In recent years, ruthenium complexes have attracted much attention as new transition-metal-based antitumor agents, as they have certain advantages over the platinum complexes that are currently used in cancer chemotherapy.[10] They show less toxicity, they are selective of tumor cells, and present a novel mechanism of action, the prospect of non-cross-resistance and a different spectrum of activity.[11–19]

In a previous study, we recently reported that complexes with the general formula [Ru(AA-H)(dppb)(bipy)]PF_6 (AA-H = amino acid anion) inhibited the growth of Ehrlich carcinoma cells in vitro.[20] Among the Ru(II)/amino acid/diphosphine complexes evaluated, those with L-methionine and L-tryptophan present the best activity against Ehrlich carcinoma cells, with IC_{50} values (concentration that results in a 50% reduction in cellular viability) of $10.2 \pm 2.3\,\mu M$ and $8.7 \pm 3.1\,\mu M$, respectively.[20]

Ehrlich carcinoma is a murine mammary adenocarcinoma, referred to as an undifferentiated carcinoma, has high transplantable capability, no-regression, rapid proliferation, shorter life span, and 100% malignancy.[21,22] The ascitic form of the tumor is widely used as an experimental model for new chemotherapeutic studies. Ehrlich ascites carcinoma (EAC) is considered similar to the human tumors which are the most sensitive to chemotherapy due to its undifferentiated feature and rapid proliferation rate.[22,23]

Thus, the aim this study was to analyze the antitumor efficacy and side effects of the [Ru(L-Met)(bipy)(dppb)]PF_6 (**1**) and the [Ru(L-Trp)(bipy)(dppb)]PF_6 (**2**) complexes (Figure 1) using the cisplatin as a reference drug, with respect to the peritoneal carcinomatosis model (EAC). The antitumor efficacy was evaluated by tumor growth inhibition, survival time, and angiogenesis inhibition. The cell death type induced by Ru(II)/amino acid/diphosphine complexes was also investigated. Our study is the first that evaluated the effect of Ru(II)/amino acid/diphosphine complexes for antitumor activity in vivo and is the first study that used chick embryo chorioallantoic membrane (CAM) model with EAC cells also.

Materials and methods

Synthesis and characterization of compounds

The synthesis and characterization of [Ru(L-Met)(bipy)(dppb)]PF_6 (**1**) and [Ru(L-Trp)(bipy)(dppb)]PF_6 (**2**) complexes were described previously by our research group.[20] Briefly, the complexes were synthesized by reacting the precursor cis-[$RuCl_2$(dppb)(bipy)] with an excess of the amino acid. The solution was refluxed and stirred, and NH_4PF_6 was added. After 1 h, the solvent was removed, dichloromethane was added, and the mixture was filtered. The volume of the solution was reduced, and ether was added; an orange solid was precipitated, isolated by filtration, washed with H_2O and diethyl ether, and dried under a vacuum, giving a yield of 85%–90%. The compounds were characterized by microanalysis, Infrared (IR), and nuclear magnetic resonance (NMR) spectroscopy and by thin layer chromatography, and the data were compared with those reported previously.[20]

In vivo studies

Animals. The 6–8 week-old Swiss albino mice with an average body weight of 25–35 g were used for the experiments. The animals were maintained under standard laboratory conditions (22–25°C with dark/light cycle, 12/12 h) and allowed free access to a standard dry pellet diet and water *ad libitum*. They were acclimatized to laboratory conditions for 5 days before the experiments.

Mouse tumor model. The Ehrlich tumor, murine mammary carcinoma, was introduced intraperitoneally (i.p.) as ascites tumors (peritoneal carcinomatosis) into the Swiss albino mice. After 7 days of cell inoculation, the peritoneal fluid of an animal with EAC was aspirated, the cells were

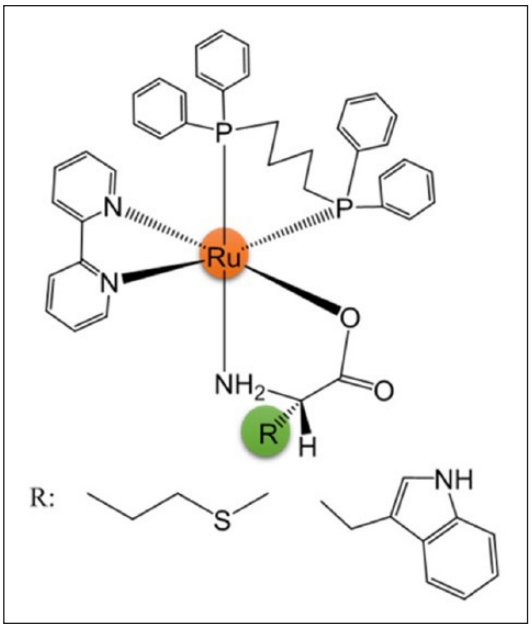

Figure 1. Structure of $[Ru(AA-H)(dppb)(bipy)]PF_6$ complexes: AA = methionine **(1);** tryptophan **(2).**

washed in sterile phosphate-buffered saline (PBS), and an aliquot of the cell suspension was put into 1% (m/v) Trypan blue (Sigma-Aldrich, St. Louis, MO, USA) and counted in a Neubauer Chamber. Only cell dilutions with ≥90% viable cells were used for both the in vitro and in vivo studies.[24]

Antitumor activity in vivo. The animals were divided into seven all-male groups of eight. They were inoculated i.p. with 6×10^6 viable EAC cells per mouse, in a volume of 0.2 mL, 24 h after the treatment was initiated. A negative control served as tumor control and received PBS, while the vehicle group was treated with PBS containing 10% dimethyl sulfoxide (DMSO; Sigma-Aldrich). A third group was treated with cisplatin, 2 mg kg^{-1} body weight. Solutions of complexes **1** and **2** were prepared in PBS containing 10% DMSO and administered to the treated group at a dose of 2 and 6 mg kg^{-1} body weight. All the treatments were given for 7 days. The EAC inhibition growth was determined from the differences between changes in abdominal circumference (ΔAC) and body weight (ΔBW) of the animals using the following equation based on a method developed by Kviecinski et al.[25] and Sunil et al.,[26] respectively

$$\%\text{Inhibition } \Delta AC = \left(\frac{\Delta AC_n - \Delta AC_t}{\Delta AC_n} \right) \times 100$$

$$\%\text{Inhibition } \Delta BWC = \left(\frac{\Delta BW_n - \Delta BW_t}{\Delta BW_n} \right) \times 100$$

where ΔAC_n and ΔAC_t are the changes in abdominal circumference from the negative and treated groups, respectively. ΔBW_n and ΔBW_t represent the body weight changes from the negative and treated groups, respectively.

The antitumor activity was classified according to the percentage of tumor growth inhibition: absent (when the percentage inhibition of tumor equals 0), mild (when the percentage of tumor inhibition ≤25%), moderate (when the percentage of tumor inhibition ≥ 26%–50%), and high (when the percentage of tumor inhibition ≥51%). Throughout the period, the animals were observed, and all behavioral changes and signs of toxicity or deaths were recorded during the first 4 h and then daily.[27]

Hematological and biochemical parameters. After 7 days of treatment, hematological and clinical chemistry examinations were performed on all surviving animals with saline solution, complexes **1** and **2,** or cisplatin. The mice were euthanized i.p. with a solution of 0.2 mL/100 g of ketamine (100 mg mL^{-1}; Dopalen; Vetbrands LTDA, Brazil) and xylazine (100 mg mL^{-1}; Dorcipec; Vallée S/A Produtos Veterinários, Brazil). Blood samples were collected in tubes containing 10% w/v ethylenediaminetetraacetic acid (EDTA) and also in tubes without anticoagulants. The hematological parameters evaluated included erythrocyte (red blood cell (RBC)) counts, hemoglobin (Hb), hematocrit (HCT), total leukocytes (white blood cell (WBC)), and platelet counts. All analyses were performed using an automated analyzer (Beckman Coulter T-890; Beckman Coulter, Inc., Brea, CA, USA). Biochemical assays were performed on serum samples to estimate urea, creatinine, aspartate aminotransferase (AST/SGOT), and alanine aminotransferase (ALT/SGPT), using an automated analyzer (VitalabFlexor XL; Vital Scientific, The Netherlands).

Histopathological examination. The liver and kidneys were removed, washed with 1× PBS and fixed in 10% (v/v) formalin. All tissues were embedded in paraffin blocks, sectioned into 5 µm in thickness and placed on glass slides. After hematoxylin–eosin staining, the slides were observed and photos were taken using an optical microscope (Carl Zeiss Axiovert w, Germany) containing AxioVision 4.8 software (Carl Zeiss).

Evaluation of the apoptosis using Annexin V–fluorescein isothiocyanate double staining by flow cytometry. After treatment, the ascitic fluid collected from the peritoneal cavity of the animals was used to determine the cell death of EAC cells by flow cytometer. The population of interest was selected, and the cells undergoing apoptosis were determined by quantification of phosphatidylserine exposure on the cell surface using staining with fluorescein isothiocyanate (FITC)-conjugated Annexin V and propidium iodide (PI; BD Biosciences, San Diego, CA, USA). A volume of 5×10^5 cells were stained with 2.5 µL of FITC-conjugated

Annexin V plus 3 μL of PI (10 mg mL^{-1}) for 15 min at room temperature in the dark. Cells were analyzed using a flow cytometer (FACSCalibur™; BD Biosciences) acquiring 10,000 events/sample using Cell Quest software. The criteria for positivity in cells at the early stages of apoptosis were Annexin V positive and PI negative, whereas the criteria for cells at the later stages of apoptosis were both Annexin V and PI positive. The criteria for cells in necrosis were Annexin V negative and PI positive. Animals which did not have ascites underwent peritoneal lavage using 9% (w/v) NaCl in order to capture the tumor cells found in the abdominal cavity for the analyses.

Assessment of apoptosis and necrosis. The ascitic fluid collected from the peritoneal cavity of the animals (n = 4 per group) was washed with PBS. A volume of 2×10^5 EAC cells were suspended in Hoechst (HO) 33342 (10 μg mL^{-1}) and PI (2.5 μg mL^{-1}) solution and then incubated at 37°C for 10 min in total darkness. The slides were observed using a fluorescence microscope (Leica, Germany). At least 300 target cells were counted for each animal (n = 4 per group). The percentages of apoptotic (early and late apoptosis) and necrotic cells were determined from the total number of cells: (1) viable—blue chromatin with organized structure, (2) early apoptosis—bright blue chromatin that is highly condensed or fragmented, (3) late apoptosis—bright pink chromatin that is highly condensed or fragmented, and (4) necrosis—pink chromatin with organized structure.[28,29]

Cell cycle analyses. In order to discriminate cell cycle phase distribution after treatment in vivo, 5×10^5 cells of the ascitic fluid were harvested by centrifugation, washed with PBS, fixed with 70% (v/v) cold aqueous ethanol, and stored overnight at −20°C. The fixed cells were then washed with PBS and incubated with PI (BD Biosciences) containing 0.05% RNase. Samples were incubated at 4°C in the dark and analyzed by flow cytometry. The percentage of cells in the sub-G1, G0/G1, S, and G2/M phases were analyzed using a flow cytometer (FACSCalibur™; BD Biosciences) acquiring 10,000 events/sample using ModFit software.

Mean survival time and increased life span. Survival was determined using the same experimental procedure for the treatment of antitumor activity. The death of the mice was noted daily up to 30 days after each treatment to determine mean survival time (MST) and percentage increase in life span (% ILS). The MST of each group was monitored by recording mortality daily for 30 days. The % ILS was calculated using the following equation[30]

$$\%\,\mathrm{ILS} = \left(\frac{\mathrm{MSt}_{\text{treated group}}}{\mathrm{MST}_{\text{negative group}}} \right) \times 100$$

where MST = Σ survival time (days) of each mouse in a group/total number of mice.[30] An enhancement of % ILS ≥25% in the control was considered as an effective antitumor response.

Chick chorioallantoic membrane angiogenesis assay. The CAM model was used to assess complexes **1** and **2** antiangiogenic activity according to a methodology adapted from Melo-Reis et al.[31] Forty fertile chicken eggs (*Gallus domesticus*) were incubated at 37°C in a humidified atmosphere (60%–70% relative humidity). On the fifth day of incubation, a circular hole was opened in the large end of the eggshell, the thin white membrane on the CAM was removed, and the eggs were returned to the incubator. On the 13th day of incubation, the eggs were divided into four treatment groups of 10 eggs each: (1) Control: water with 1% DMSO, (2) EAC cells (6×10^5 cells per CAM), (3) complex **1** ($IC_{50:}$ 10 μM[20]) co-treated with EAC cells, and (4) complex **2** ($IC_{50:}$ 10 μM[20]) co-treated with EAC cells. It was placed on top of the CAM, under sterile conditions, 50 μL of each of these solutions in the indicated concentrations, and, after 72 h, the angiogenic response was evaluated. CAMs were fixed in formaldehyde solution (3.7%) for 5 min, cut with curved blunt scissors, and maintained in Petri plates with formaldehyde solution. Analysis and quantification of newly formed vascular net were made through captured images. The percentage area of each assay was determined using the GIMP 2.8 and ImageJ 1.49 software. Images were prepared so that saturation, light, and contrast allowed a better resolution of the blood vessels which were quantified in corresponding pixels.[31]

In vitro studies

Cell culture. EAC cells were aspirated from the peritoneal cavity of the animals and washed with1× PBS solution, and then maintained in a humidified atmosphere (Thermo Fisher Scientific, Waltham, MA, USA) for 24 h at 37°C in 5% CO_2. RPMI-1640 medium was supplemented with 10% fetal calf serum, 100 IU mL^{-1} penicillin G, and 100 μg mL^{-1} streptomycin (Sigma-Aldrich).

Western blot assay. To evaluate whether complexes **1** and **2** induce caspase-mediated cell death in EAC cells, 2×10^6 cells were treated with compounds at IC_{50} values approximately (10 μM) for 24 h. Total cellular proteins were extracted by incubating the cells in lysis buffer obtained from Invitrogen. Protein concentrations were determined by Bradford assay. Equal amounts of protein were loaded per lane in 12% sodium dodecyl sulfate–polyacrylamide gel electrophoresis (SDS-PAGE) as described previously.[17] After electrophoresis, separated proteins were transferred onto nitrocellulose membranes and blocked with 5% nonfat milk in Tris-buffered saline with Tween 20 (TBST) buffer for 1 h at room temperature. Afterward, the membranes were incubated with primary specific antibodies for caspase 3 and glyceraldehyde 3-phosphate dehydrogenase (GAPDH). The GAPDH antibody was used as control. All

Table 1. Antitumor activity of Ru(II)/amino acid/diphosphine complexes against EAC-bearing Swiss mice according to abdominal circumference and body weight.

Group (n = 8)	Treatment	Abdominal circumference		Body weight	
		ΔAC[a] (cm)	Tumor inhibition (%)	ΔBW[b] (g)	Tumor inhibition (%)
Negative[c]	PBS	2.14 ± 0.20	–	10.64 ± 1.06	–
Vehicle	DMSO	2.04 ± 0.22	–	8.27 ± 0.95	9.13 ± 3.43
Complex 1	2 mg kg^{-1}	0.49 ± 0.30[d***,e**]	68.62 ± 14.97[e***]	5.06 ± 0.84[d**]	52.41 ± 7.93[e**]
	6 mg kg^{-1}	0.69 ± 0.32[d**,e**]	68.07 ± 15.09[e***]	5.00 ± 0.92[d***]	50.47 ± 9.06[e*]
Complex 2	2 mg kg^{-1}	0.95 ± 0.27[d*,e*]	65.42 ± 10.09[e**]	6.10 ± 0.68[d*]	47.68 ± 4.71[e*]
	6 mg kg^{-1}	0.33 ± 0.16[d***,e***]	84.42 ± 7.70[e***]	3.76 ± 0.92[d***]	74.62 ± 6.46[e***]
Cisplatin	2 mg kg^{-1}	0.26 ± 0.11[d***,e***]	87.73 ± 5.22[e***]	3.96 ± 0.43[d***]	62.79 ± 4.08[e*]

EAC: Ehrlich ascites carcinoma; ΔAC: changes in abdominal circumference; ΔBW: changes in body weight; PBS: phosphate-buffered saline; DMSO: dimethyl sulfoxide.
Data show mean ± SEM.
[a]Variation in abdominal circumference.
[b]Variation in body weight.
[c]Negative control group.
[d]Normal group versus negative group.
[e]Normal group versus vehicle group.
*p < 0.05; **p < 0.01; ***p < 0.001.

antibodies were diluted according to manufacturer's instructions (Cell Signaling Technology, Danvers, MA, USA) and incubated at 4°C for ovvernight. The immunoreactive bands were detected using an enhanced chemiluminescence (ECL) western blotting substrate (Super Signal West Pico Substrate; Thermo Fisher Scientific), and the ECL signals were captured using a CCD camera (ImageQuant LAS 4000 mini; GE Healthcare, Chicago, IL, USA). The optical density of the target protein bands was measured using ImageJ 1.49 software to compare the protein levels.

Glucose uptake assay. To verify whether glucose uptake can be modified by the presence of complexes **1** and **2**, 1×10^5 EAC cells were treated with or without compounds at IC_{50} values approximately (10 μM) for 48 h, in triplicate. After treatment, the conditioned medium was collected, and the glucose concentration was measured using an automated analyzer (VitalabFlexor XL, Vital Scientific) modified by Fu et al.[32]

Evaluation of competitive inhibition. To evaluate responses to the system L competitive inhibitor, 2-aminobicyclo-(2,2,1)-heptane-2-carboxylic acid (BCH; Sigma-Aldrich), 1×10^5 EAC cells were treated with or without 5 μM of BCH in 1N NaOH. Complexes **1** and **2** in different concentrations (5, 10, and 20 μM) were added 15 min after BCH, and the control cultures received an equivalent concentration of NaOH. Cells were treated with BCH/Ru(II) complexes for 4 h after which the treatment medium was removed and replaced with fresh media, adapted by Lin et al.[33] Finally, 24 h later, the cells were counted using an automated cell counter (Luna Automated Cell Counter; Logos Biosystems, Annandale, VA, USA) to determine the ratio of live to dead cells. All experiments were performed in triplicate.

Statistical analysis

Data were analyzed for statistically significant experimental differences using an analysis of variance (ANOVA) followed by the Tukey or Bonferroni test. Statistical significance was considered at $p < 0.05$. All statistical analyses were performed using the statistical software GraphPad Prism, version 5 for Windows (GraphPad Software Inc., La Jolla, CA, USA).

Results

Peritoneal carcinomatosis inhibition and clinical symptoms

The antitumor activities of complexes **1** and **2** were tested in EAC-bearing mice, and the analysis of tumor growth inhibition by ΔAC showed high antitumor potential for these complexes (Table 1). The analysis of tumor growth inhibition by ΔBW against EAC cells showed antitumor activity ranging from moderate to high. Cisplatin exhibited high potential tumor growth inhibition, with the two methods used: ΔAC and ΔBW (Table 1).

The animals treated for 7 days with complexes **1** and **2** (2 and 6 mg kg^{-1}) showed no signs of toxicity or change in behavior. Treatment with complex **1** (2 mg kg^{-1}) caused mild writhing in two animals over the first 30 min but subsequently this sign was not observed. The animals treated with cisplatin showed alopecia, diarrhea, discreetly modified

Table 2. Effect of Ru(II)/amino acid/diphosphine complexes on the hematological parameters in peripheral blood of EAC-bearing mice.

Group (n = 8)	Treatment	Total leukocytes (WBC; 10^3/mm^3)	Erythrocyte (RBC) counts (10^6/mm^3)	Hb (g/dL)	HCT (%)	Platelets (10^3/mm^3)	Lymphocytes (%)
Normal[a]	–	6.9 ± 0.6	9.4 ± 0.1	13.6 ± 0.2	41.2 ± 0.8	810 ± 55	73.1 ± 1.6
Negative[b]	PBS	5.0 ± 0.9	5.7 ± 0.5[c**]	9.4 ± 1.0[c*]	302 ± 2.8[c*]	716.7 ± 92.4	65.40 ± 4.61
Vehicle	DMSO	4.6 ± 0.4	5.2 ± 0.6[c**]	9.4 ± 1.0[c*]	27.9 ± 3.4	564.8 ± 190.1	58.42 ± 10.72
Complex 1	2 mg kg^{-1}	6.7 ± 1.3	5.6 ± 0.9	10.5 ± 1.4	30.1 ± 5.1	583.1 ± 73.4	41.13 ± 8.18
	6 mg kg^{-1}	5.8 ± 0.7	4.8 ± 0.3	8.8 ± 0.6	25.6 ± 1.8	334.8 ± 93.2[d***]	58.05 ± 5.84
Complex 2	2 mg kg^{-1}	8.1 ± 0.4	6.1 ± 0.6	10.9 ± 1.0	33.0 ± 3.5	837.6 ± 187.6	51.07 ± 6.24
	6 mg kg^{-1}	5.5 ± 0.8	7.5 ± 0.4	12.5 ± 0.8	39.3 ± 2.3	1218.7 ± 130.1[d***]	70.10 ± 2.86
Cisplatin	2 mg kg^{-1}	2.1 ± 0.4	3.4 ± 0.9	6.4 ± 1.2	17.6 ± 4.7	279.6 ± 75.7[d***]	80.65 ± 1.33

EAC: Ehrlich ascites carcinoma; WBC: white blood cell; RBC: red blood cell; Hb: hemoglobin; HCT: hematocrit; PBS: phosphate-buffered saline; DMSO: dimethyl sulfoxide.
[a]Reference values.[34]
[b]Negative control group.
[c]Normal group versus negative control and vehicle groups.
[d]Normal group versus negative control group.
*$p < 0.05$; **$p < 0.01$; ***$p < 0.001$.

Table 3. Effect of Ru(II)/amino acid/diphosphine complexes on the biochemical parameters in peripheral blood of EAC-bearing mice.

Group (n = 8)	Treatment	Urea (mg/dL)	Creatinine (mg/dL)	AST/TGO (U/L)	ALT/TGP (U/L)
Normal[a]	–	47 ± 4	0.4 ± 0.0	277 ± 18	62.0 ± 4
Negative[b]	PBS	52.5 ± 3.4	0.4 ± 0.2	933.7 ± 140.7[c***]	739.2 ± 104.2[c***]
Vehicle	DMSO	59.1 ± 5.4	0.5 ± 0.1	812 ± 181[c***]	763 ± 73[c***]
Complex 1	2 mg kg^{-1}	51.3 ± 1.1	0.3 ± 0.1	1150 ± 232	139.6 ± 16.9[d***]
	6 mg kg^{-1}	60.2 ± 2.7	0.2 ± 0.1	1291 ± 195	132.5 ± 14.4[d***]
Complex 2	2 mg kg^{-1}	59.0 ± 3.6	0.4 ± 0.1	1964 ± 251[d**]	177.0 ± 26.0[d***]
	6 mg kg^{-1}	58.1 ± 4.5	0.4 ± 0.1	1374 ± 236	128.6 ± 22.6[d***]
Cisplatin	2 mg kg^{-1}	56.0 ± 2.8	0.3 ± 0.1	1577 ± 344	815 ± 25.3

EAC: Ehrlich ascites carcinoma; AST: aspartate aminotransferase; ALT: alanine aminotransferase; PBS: phosphate-buffered saline; DMSO: dimethyl sulfoxide.
[a]Reference values.[34]
[b]Negative control group.
[c]Normal group versus negative control and vehicle groups.
[d]Normal group versus negative control group.
**$p < 0.01$; ***$p < 0.001$.

muscle tone, and moderate ataxia throughout the 7-day treatment. No deaths were recorded during the treatment period.

Evaluation of hematological, biochemical, and histopathological parameters

Induction of the EAC changed the hematological and biochemical parameters of the mice (Tables 2 and 3). The values of erythrocytes, Hb, and HCT obtained from the negative control and vehicle groups were lower than the reference values for Swiss male tumor-free mice.[34] In addition, there were increased values of AST/SGOT and ALT/SGPT in the animals in the negative control and vehicle groups. Animals treated with complexes **1** and **2** statistically altered the platelet count (Table 2). The treatment with complex **1** (6 mg kg^{-1}) and cisplatin (2 mg kg^{-1}) caused a decrease in the number of platelets, while complex **2** (6 mg kg^{-1}) caused an increase in the platelet count of the mice. The histological analysis of the experimental groups showed liver and kidney changes (Figures 2 and 3). The livers of tumor-free animals showed no sign of necrosis, fatty degeneration, or inflammation, while the livers of all animals in the experimental groups showed mild cellular infiltration. However, glomerular structures and proximal and distal tubules in the mice kidneys were normal. Only the kidneys of animals treated with complex **1** (2 and 6 mg kg^{-1}) showed congestion and mild tubular necrosis. Furthermore, a microscopic examination of the kidney of one animal only showed that tumor cells had adhered to the organ capsule after treatment

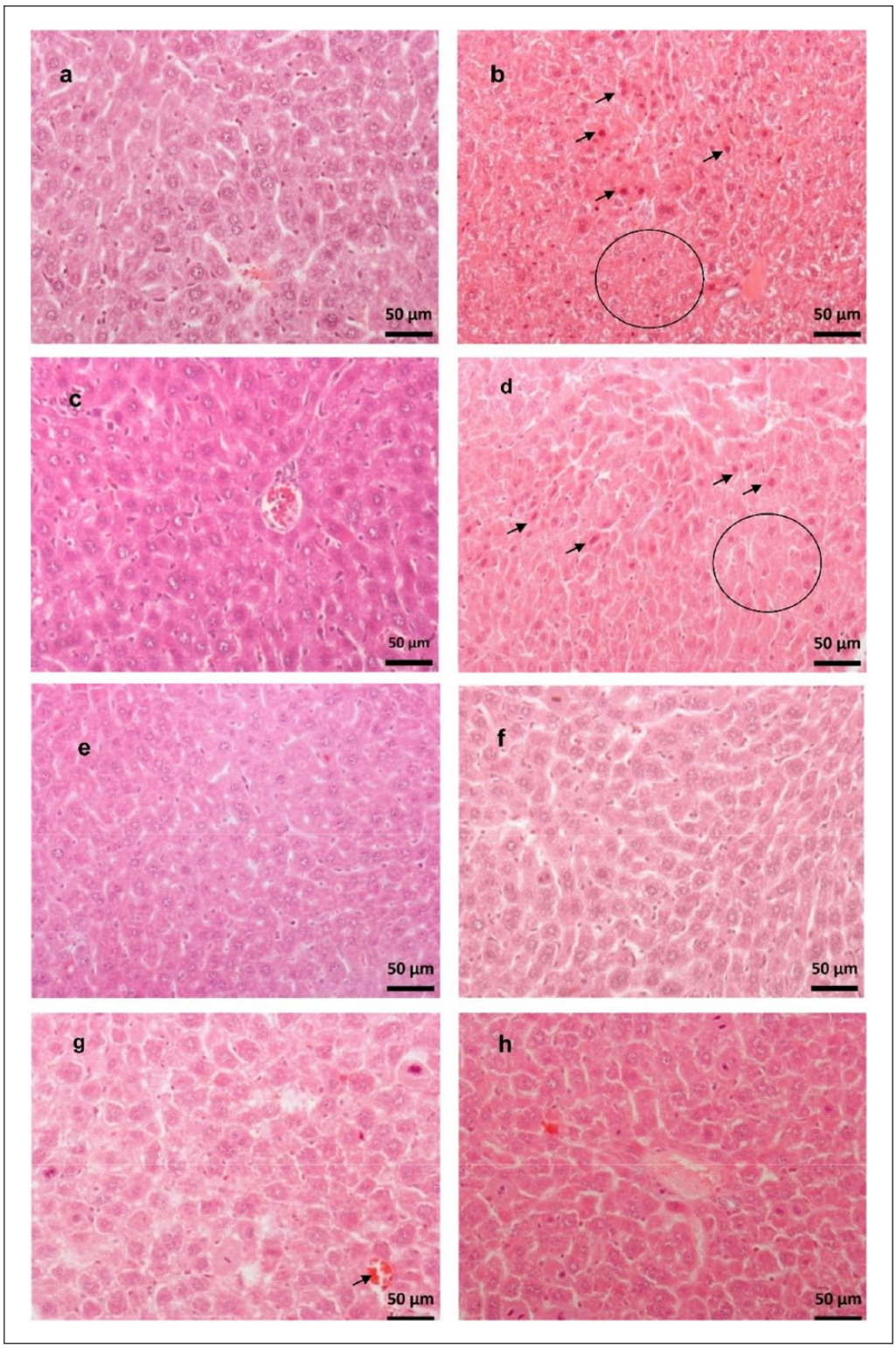

Figure 2. Effect of Ru(II)/amino acid/diphosphine complexes on the histopathological parameters of the livers of EAC-bearing mice. (a) Normal—hepatocytes with normal appearance and unchanged tissue. (b) Negative control—mild necrosis (circle) with eosinophilic hepatocytes with pyknotic nuclei (arrows) and cellular inflammation. (c) Vehicle—hepatocytes with normal appearance and mild cellular inflammation. (d) Cisplatin ($2\,mg\,kg^{-1}$)—mild necrosis (circle) with eosinophilic hepatocytes with pyknotic nuclei and cariorrexis (arrows), liver with mild cellular inflammation. (e) Complex **1** ($2\,mg\,kg^{-1}$)—hepatocytes with normal appearance and mild cellular inflammation. (f) Complex **1** ($6\,mg\,kg^{-1}$)—hepatocytes with normal appearance and mild cellular inflammation. (g) Complex **2** ($2\,mg\,kg^{-1}$)—hepatocytes with normal appearance and mild cellular inflammation. (h) Complex **2** ($6\,mg\,kg^{-1}$)—mild cellular inflammation.

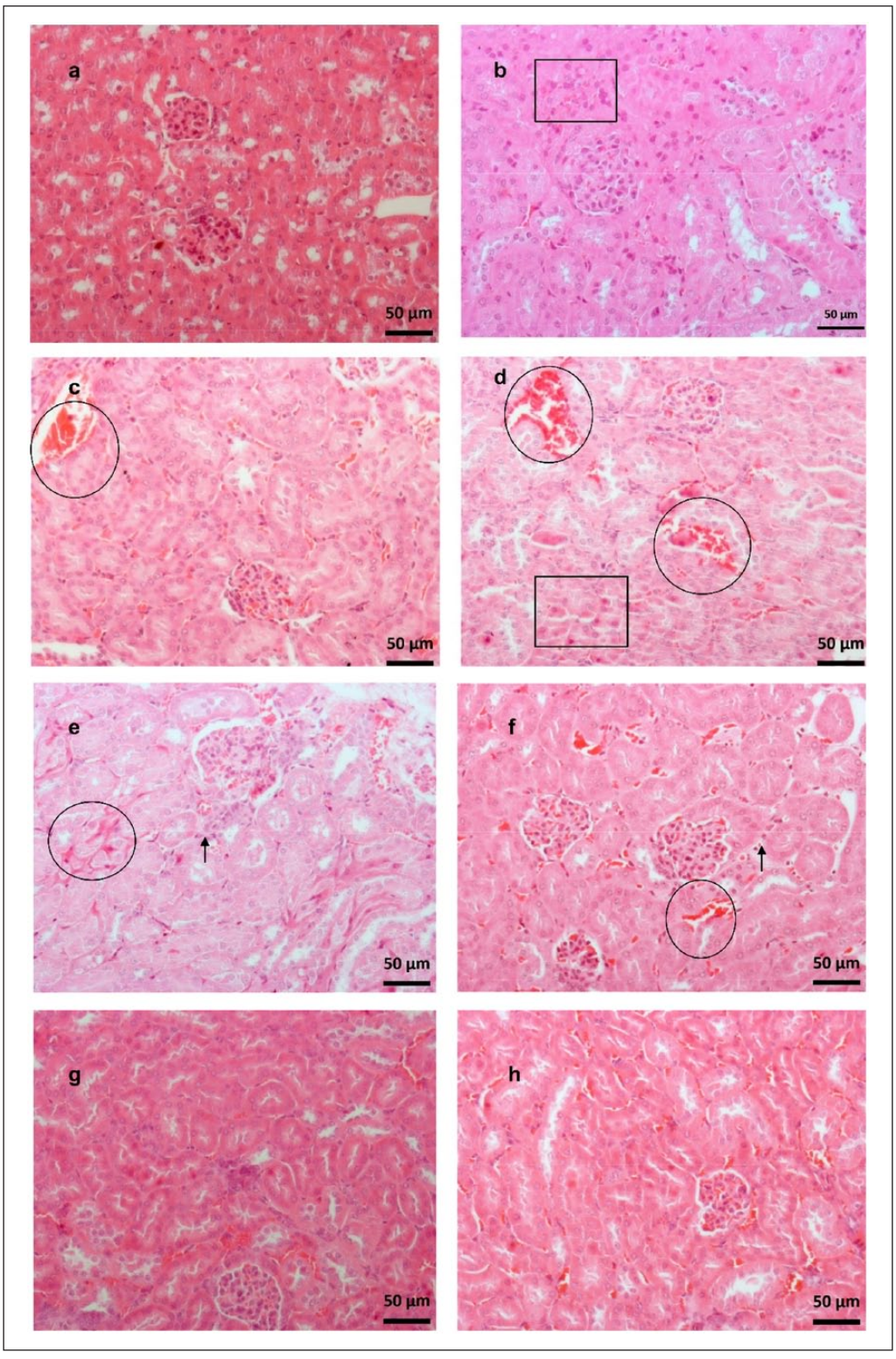

Figure 3. Effect of Ru(II)/amino acid/diphosphine complexes on the histopathological parameters of the kidneys of EAC-bearing mice. (a) Normal—renal cells with normal appearance and unchanged tissue. (b) Negative control—mild tubular necrosis (square) and tissue congestion. (c) Vehicle—mild tubular necrosis, hyperemia (circle), and tissue congestion. (d) Cisplatin (2 mg kg^{-1})—mild to moderate necrosis (square) with eosinophilic renal cells with pyknotic nuclei and cariorrexis and intensive hyperemia (circle). (e) Complex **(1)** (2 mg kg^{-1})—mild tubular necrosis, hyperemia (circle), mild cellular inflammation (arrows), and tissue congestion. (f) Complex **(1)** (6 mg kg^{-1})—mild tubular necrosis, hyperemia (circle), mild cellular inflammation (arrows), and tissue congestion. (g) Complex **(2)** (2 mg kg^{-1})—renal cells with normal appearance and unchanged tissue. (h) Complex **(2)** (6 mg kg^{-1})—renal cells with normal appearance and unchanged tissue.

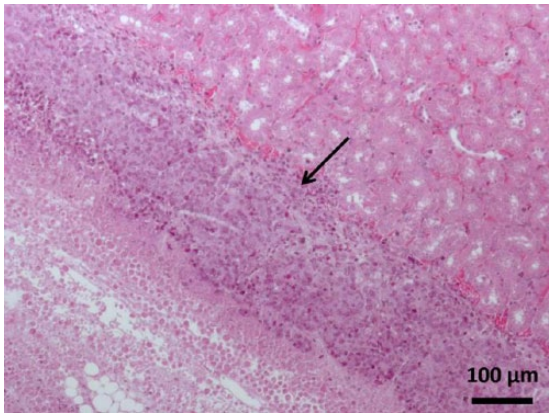

Figure 4. Tumor cells adhered to the kidney capsule (arrow) and marked hyperemia, tissue congestion, and cellular inflammation.

with a 2 mg kg^{-1} dose of complex **1** (Figure 4). Treatment with cisplatin caused mild inflammation, congestion, and necrosis in the liver and moderate inflammatory infiltrate and mild necrosis in the kidneys.

Effect of complexes 1 and 2 on the reduction of tumor cell viability and cell death in vivo

The cell death type induced by complexes **1** and **2** was evaluated by measuring the number of Annexin V positive, activated caspase-3 levels, and morphological features. The externalization of phosphatidylserine in cellular membrane was determined by number of Annexin V positive cells using flow cytometer. As shown in Figure 5(a), although animals from the negative control and vehicle groups presented a percentage of viable cells of about 91%, animals treated with complexes **1** and **2** (2 and 6 mg kg^{-1}) showed a lower percentage of viable cells, varying from 75.6% to 84.8%, and a simultaneous increase in the percentage of non-viable cells. Treatment with complex **1** (2 mg kg^{-1}) induced the death of EAC cells by late apoptosis (11.1% ± 3.1%, $p < 0.05$) when compared to the negative control group. All treatments were capable of increasing the percentage of apoptotic death when compared with the negative control and vehicle groups. These results suggest that the complexes induced decrease in cell viability, probably inducing apoptosis.

To confirm the type of cell death induced by compounds, the cleavage of caspase-3 was investigated by western blotting and morphological analysis was analyzed using the HO/PI double staining. As shown in Figure 5(b) the protein levels of caspase-3 were significantly increased in response to both treatments. EAC cells with complex **1** increased cleaved caspase-3 protein levels by 1.4 ± 0.1-fold ($p < 0.05$), and when exposed to complex **2,** higher protein levels were clearly observed (2.7 ± 0.3-fold, $p < 0.001$).

The typical morphological features of apoptosis and necrosis were considered: apoptosis—nuclear condensation, cell shrinkage, membrane blebbing, and DNA fragmentation; and necrosis—swollen enlarged cells with disintegrated cell membrane (Figure 5(c)). Both compounds, when tested, caused cell death by apoptosis (Figure 5(d)). The treatment with complex 1 at doses of 2 and 6 mg kg^{-1} bw induced apoptosis in 29% ± 5% ($p < 0.001$) and 19% ± 4% ($p < 0.01$) of the EAC cells, respectively. While, 23% ± 7% ($p < 0.001$) and 23% ± 2% ($p < 0.001$) of EAC cells collected from animals treated with complex 2 (2 and 6 mg kg^{-1} bw, respectively) also undergo apoptosis.

Effect of complex 1 and 2 on cell cycle kinetics

Treatment of the negative control group with saline showed that most cells were viable, with a typical distribution in the sub-G1, G0/G1, S, and G2/M phases (Figure 6). However, after treatment of the mice with complexes **1** and **2**, there was a change in the cell cycle, when compared to the negative control group, with an increase in the percentage of cells in sub-G1 and G0/G1 and a consequent reduction in cells in the S and G2/M phases (Figure 6).

MST and ILS

The survival rate of EAC-bearing mice treated with complexes **1** and **2** was determined by daily observations: deaths were recorded over a 30-day period. Survival rate was represented by the Kaplan–Meier curve (Figure 7). As demonstrated in Table 4, negative control and vehicle groups showed an MST of 18 and 19.6 days, respectively. The MST of complexes **1** and **2** (2 and 6 mg kg^{-1}) ranged from 23.6 to 27.4 days, with a significant statistical difference between the negative control and vehicle groups. Treatment of mice with cisplatin showed an MST of 21 days. All treatments with complexes **1** and **2** increased the life span of EAC-bearing mice (% ILS ≥ 25; Table 4). Animals treated with cisplatin did not show any significant ILS (% ILS = 17).

Antiangiogenic activity in the CAM model and glucose uptake in vitro

Angiogenesis is critical to cancer progression because new blood vessels provide nutrition and oxygen, and elimination of accumulated metabolic wastes.[35,36] CAM model is an attractive model to rapidly evaluate the efficacy of novel therapeutic drug and the in vivo inhibition of several tumor types.[37] As shown in Figure 8, the EAC cells induced angiogenesis in the CAM model with vascularization percentage of 34% ± 5% ($p < 0.001$ compared to control). The

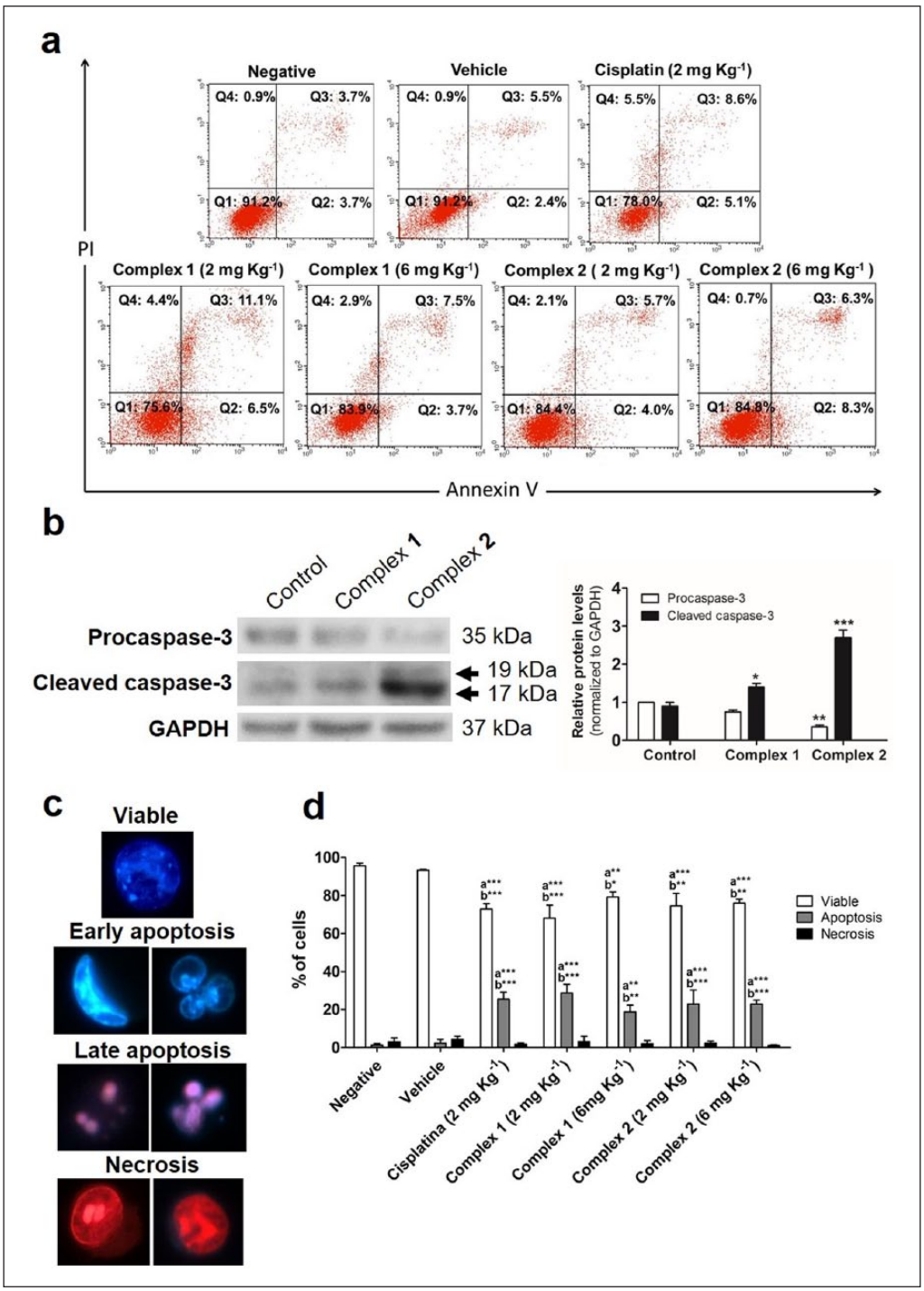

Figure 5. Effect of Ru(II)/amino acid/diphosphine complexes on the mechanism of cell in Ehrlich ascites carcinoma cells after treatment of EAC-bearing mice. (a) Flow cytometric analysis using the Annexin V–FITC/PI double staining: Q1—viable cells, Q2—Annexin V+/PI−, Q3—Annexin V+/PI+, Q4—Annexin−/PI+. Data show the mean ± SEM of eight animals per treatment. (b) Western blot analysis of caspase-3 protein levels in EAC cells after incubation with complexes **1** and **2** for 24 h. GAPDH immunoblotting is a loading control. Quantitative analysis of protein expression using ImageJ software. Graphs show quantification of protein expression after normalizing the data (*$p < 0.05$, **$p < 0.01$, and ***$p < 0.001$ indicate statistically significant differences with the untreated control). (c) Representative images show morphological changes of EAC cells detected with dual staining of Hoechst 33342/PI: viable—blue chromatin with organized structure, necrosis—red chromatin with organized structure, early apoptosis—bright blue chromatin highly condensed or fragmented, and late apoptosis—pink or red chromatin highly condensed or fragmented. (d) Percentage of EAC cells in apoptosis and necrosis after treatment of EAC-bearing mice by double staining with HO/PI. Data show the mean ± SEM of four animals per treatment ('a' vs negative group, 'b' vs vehicle group; *$p < 0.05$, **$p < 0.01$, and ***$p < 0.001$ indicate statistically significant differences with the untreated control).

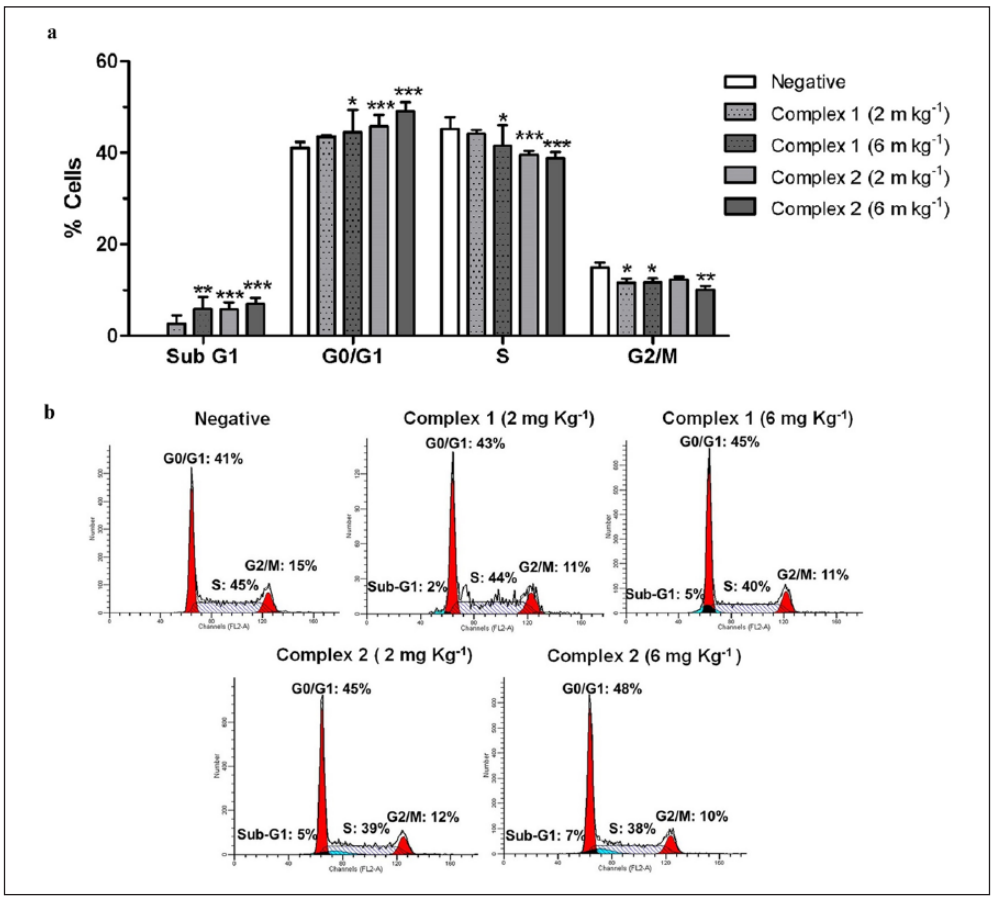

Figure 6. Effect of Ru(II)/amino acid/diphosphine complexes on cell cycle progression in Ehrlich ascites carcinoma cells after treatment of EAC-bearing mice was evaluated by flow cytometry. (a) Data show the mean ± SEM of eight animals per treatment (*$p < 0.05$, **$p < 0.01$, and ***$p < 0.001$ indicate statistically significant differences with the negative control). (b) A histogram for the cell cycle kinetics of the tumor cell in response to treatment with complexes **1** and **2** in vivo. The histogram shows the DNA content (x-axis; PI fluorescence) versus number of positive events (y-axis).

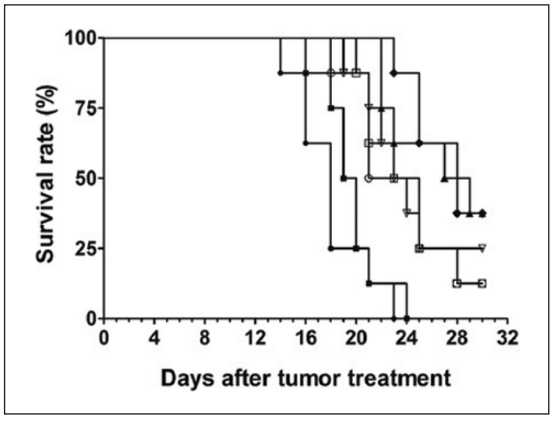

Figure 7. Effect of Ru(II)/amino acid/diphosphine complexes on the Kaplan–Meier survival estimate of EAC-bearing mice. After EAC inoculation (6×10^6 cells/mouse i.p.), mice were treated with different doses of Ru(II)/amino acid/diphosphine complexes. Animals (male; n = 8) were monitored daily for 30 days. negative group, vehicle group, complex **1** (2 mg kg^{-1}), complex **1** (6 mg kg^{-1}), complex **2** (2 mg kg^{-1}), complex **2** (6 mg kg^{-1}), and cisplatin (2 mg kg^{-1}).

co-treatment of the EAC cells with complexes **1** and **2** demonstrated that these complexes led to reduction of angiogenesis induced by EAC cells (Figure 8). The control group showed 22% ± 6% of vascularization, and the treated groups showed similar values to control, 26% ± 4% and 27% ± 4%, for complexes **1** and **2**, respectively.

To investigate whether antiangiogenic activity can change the glucose consumption, EAC cells were treated with complexes **1** and **2** for 48 h in vitro. The treatment with complexes **1** and **2** led to a decrease in glucose uptake by EAC cells after treatment compared to non-treated tumor cells (Figure 9). The cells required 37 ± 2 mg dL^{-1} and 21 ± 4 mg dL^{-1} of glucose when treated with complexes **1** and **2**, respectively, while the control required 62 ± 4 mg dL^{-1}.

Effect of the inhibition of LAT1 on the viability of tumor cells in vitro

The neutral amino acid transporter, LAT1, can regulate cell proliferation and cancer progression, such as cell

Table 4. Effect of Ru(II)/amino acid/diphosphine complexes on the MST and ILS of EAC-bearing mice.

Group (n = 8)	Treatment	MST (days)	ILS (%)	Death
Negative[a]	PBS	18	–	8
Vehicle	DMSO	19.6	9	8
Complex 1	2 mg kg^{-1}	26.6[b***,c***]	48	5
	6 mg kg^{-1}	24.3[b***,c***]	35	6
Complex 2	2 mg kg^{-1}	27.4[b***,c***]	52	5
	6 mg kg^{-1}	23.6[b***,c***]	31	7
Cisplatin	2 mg kg^{-1}	21	17	7

EAC: Ehrlich ascites carcinoma; MST: mean survival time; ILS: increase in life span; PBS: phosphate-buffered saline; DMSO: dimethyl sulfoxide. Animals (male) are monitored daily for 30 days.
[a]Negative control group.
[b]Normal group versus negative control group.
[c]Normal group versus vehicle group.
***$p < 0.001$.

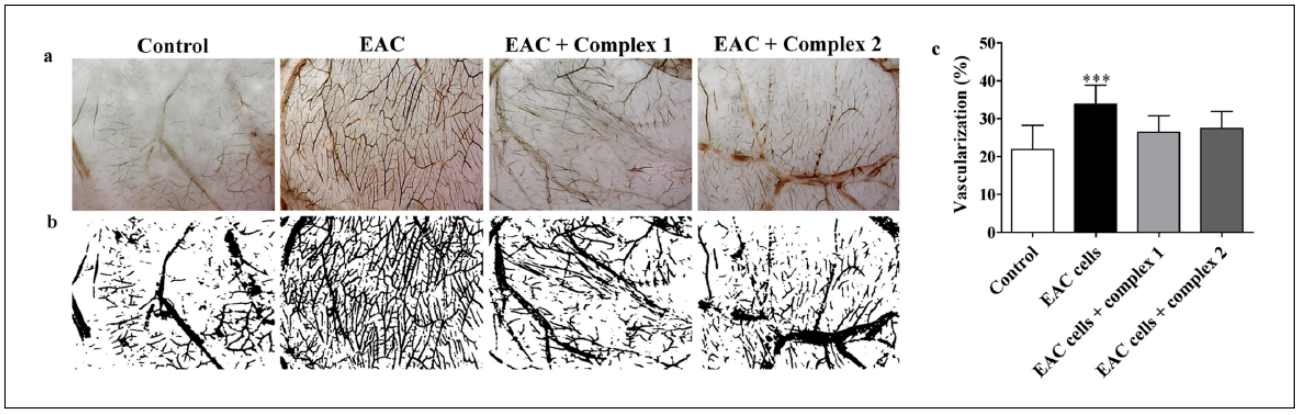

Figure 8. Antiangiogenic potential of Ru(II)/amino acid/diphosphine complexes. (a) Representative photomicrographs of different CAMs after 72 h of treatment with complexes **1** and **2**. (b) Images obtained from ImageJ software of CAMs after preparation for vascularization measure. (c) Quantification of angiogenic response of the complexes **1** and **2** co-treated with tumor cells. The percentage of vascularization from CAMs was analyzed by ImageJ software. Data show the mean ± SD of 10 CAMs per treatment (***$p < 0.001$ indicate statistically significant differences with the control (water solution in 1% DMSO)). Ehrlich ascites tumor (EAC) cells were used as angiogenesis inductor at concentration of 6×10^5 cells.

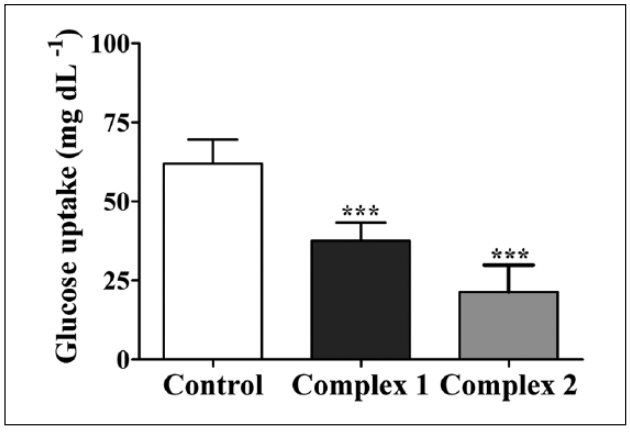

Figure 9. Effect of Ru(II)/amino acid/diphosphine complexes on the glucose consumption of Ehrlich carcinoma cells after treatment for 48 h at IC_{50} values in vitro.

growth, invasion, and angiogenesis.[38] In order to verify whether the in vitro[18,20] and in vivo effects of the Ru(II)/amino acid/diphosphine complexes observed for EAC cells could be related to the LAT1, the cells were treated with complexes **1** and **2,** in the presence and/or absence of BCH, in vitro. As shown in Figure 10, treatment with the competitive and selective inhibitor, BCH (5 μM), alone did not result in any significant differences in total number of cells or ratio of cells (live/dead). EAC cells were sensitive to therapeutic concentrations of complexes **1** and **2** (5–20 μM), yielding significant decreases in the total cell number ($p < 0.001$) and ratio of cells (live/dead; $p < 0.01$ and $p < 0.001$). The complex **1** showed effect in a non-concentration-dependent manner because when the concentration was increased, unlike expected, the total cell number and ratio of cells were also increased. Otherwise, the same effect is not observed at 5 and 10 μM of complex **2**, like

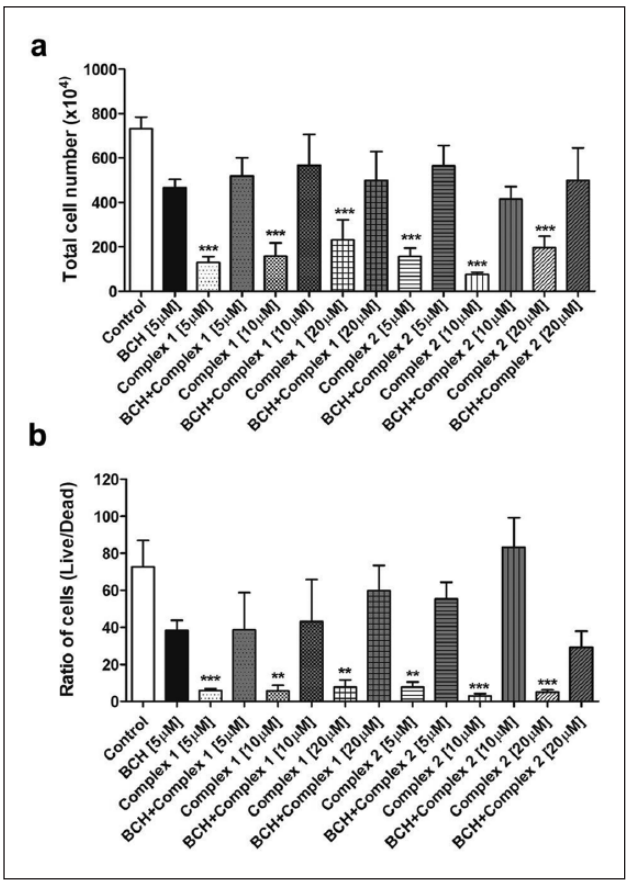

Figure 10. Effect of Ru(II)/amino acid/diphosphine complexes on the viability of Ehrlich carcinoma cells after inhibition of LAT1 in vitro. (a) Total Ehrlich tumor cell number after exposure to BCH and Ru(II)/amino acid/diphosphine complexes. (b) Ratio of cells (live/dead) after exposure to BCH and Ru(II)/amino acid/diphosphine complexes. All experiments were repeated in triplicate. Data show the mean ± SD (*$p < 0.05$, **$p < 0.01$, and ***$p < 0.001$ indicate statistically significant differences with the untreated control).

expected, the cell viability decreased with increasing concentration (Figure 10). However, this did not happen at the highest concentration of complex **2**. Those facts can be observed probably due the transporter and compound properties. Because simultaneous treatment with BCH decreased sensitivity to complexes **1** and **2**, yielding total cell numbers ($p > 0.05$) and ratio of cells (live/dead; $p > 0.05$) similar to those of the control (Figure 10).

Discussion

In this study, the antitumor effects of complexes **1** and **2** were assessed using EAC-bearing Swiss mice. These complexes were selected from among others with amino acids, using the same formula, because they have higher molecular weight and show better cytotoxic effects toward Ehrlich carcinoma cells,[20] as previously mentioned.

Complexes **1** and **2** showed high effectiveness with antitumor activity ranging from a moderate to high (Table 1) and a higher MST and increased life span (Table 4). Prolongation of an animal's life span has been considered a reliable criterion for the antitumor efficacy of new prototypes.[15,39] In this study, the clinical symptoms and hematological, biochemical, and histopathological parameters were analyzed to evaluate possible toxicological effect from treatment in EAC-beating mice. The treatment with complexes **1** and **2** did not induce any behavioral change, signs of toxicity, or animal deaths during the evaluation of antitumor activity.

As demonstrated by other similar signs of toxicity studies with cisplatin,[40,41] the results obtained for the antitumor evaluation with $2\,mg\,kg^{-1}$ of cisplatin demonstrated high therapeutic potential (Table 1). However, the treatment triggered various side effects in the EAC-bearing mice, such as weakness. Treatment of the mice led to an MST of 21 days ($p > 0.05$) and an ILS of 17% (Table 4), which were not effective for prolonging the life span.

Progression of Ehrlich carcinoma has been reported in the literature by means of hematological changes, such as a decrease in Hb and the erythrocyte count,[15,25,39] and the same were observed in our data (Table 2). The values of erythrocytes, Hb, and HCT obtained from the negative control and vehicle groups were reduced, when compared to values for Swiss male tumor-free mice (Table 2). The reduced values of erythrocytes, Hb, and HCT suggest anemia in EAC-bearing mice. Anemia seen in EAC-bearing mice is reported mainly through a reduction in erythrocytes or Hb.[42] Although the treatments with complexes **1** and **2** presented slightly increased values in the abovementioned parameters, cisplatin was able to reduce these counts in relation to normal, negative control, and vehicle groups.

Disorders in bone marrow cells have been reported after using metallodrugs, such as cisplatin and carboplatin, causing myelotoxicity,[43] while after treatment with ruthenium complexes, hematologic toxicity due to erythropenia and leukopenia were reported.[24,44] The leucocyte count for animals treated with complexes **1** and **2** showed increased values in relation to the negative control and vehicle groups, yielding values close to those of the normal group. Platelet counts were lower after treatment with complex **1** ($6\,mg\,kg^{-1}$) and higher after treatment with complex **2** ($6\,mg\,kg^{-1}$), when compared to the normal groups and negative control. Treatment with cisplatin decreased the leukocytes and platelets in relation to the normal group and negative control (Table 2), which suggests myelotoxicity, as reported in the literature.[41]

Although modifications in kidney tissue were observed in the treatment with complex **1**, the analysis of biochemical parameters did not show any significant changes in the levels of urea or creatinine (Table 3). There was an increase in both transaminases in all the experimental groups compared to the normal group, but the levels of ALT/TGP for

the groups treated with complexes **1** and **2** were lower than those found in negative control, vehicle, and cisplatin groups. However, the histological analysis revealed that all experimental groups had liver toxicity with mild inflammation and necrosis. It is most likely that the inflammation in the liver of the animals was related to the induction of EAC cells and not to drug-induced hepatitis.

According to the data obtained here, complex **2** showed greater effectiveness and safety than complex **1.** This could be attributed to the presence of the tryptophan, whose structure contains two aromatic rings and consequently has a higher molecular weight. For i.p. treatment of peritoneal carcinomatosis, drugs with a high molecular weight are more desirable because low molecular weight drugs, such as cisplatin, can be rapidly absorbed by systemic circulation, leading to decreased efficacy and increased risk of systemic toxicity, as observed in intravenous administration.[6,7]

Studies with ruthenium complexes found that the most lipophilic complexes exhibited the best cytotoxicity and highest cellular uptake.[45–47] The partition coefficient (log p) between the water or buffer and n-octanol is the most widely used measure of chemical compound lipophilicity[48] as it is a major structural factor governing both the pharmacokinetics and pharmacodynamics of drugs, because up to a certain limit, compounds with higher lipophilicity have higher permeation across biological membranes (but lower aqueous solubility). Generally, for an effective anticancer drug to initiate cell death, it must reach viable cells in a tumor and be retained at a sufficient concentration on a relevant time scale. The partition coefficient values for complexes **1** and **2** are 0.4 and 0.6, respectively.[20] Maybe the higher molecular weight of complex **2** and its enhanced lipophilicity result in its greater effectiveness and safety than complex **1**, as previously mentioned.

Studies in vitro have reported the effects of Ru(II)/amino acid/diphosphine complexes on the mechanism of growth inhibition of tumor cells.[17,18] It was found that the Ru(II)/glycine/diphosphine complexes induce apoptosis in 180 tumor sarcoma cells, as well as increases the number of Annexin V positive cells and causes G0/G1 phase cell cycle arrest, loss of mitochondrial membrane potential, activates caspase-3, caspase-8, and caspase-9, and causes a change in the messenger RNA (mRNA) expression levels of caspase-3, caspase-9 and Bax. It also increases the levels of the pro-apoptotic Bcl-2 family protein Bak.[17] For EAC cells, an in vitro study reported that Ru(II)/tryptophan/diphosphine complex (complex **2**, in this study) induces apoptosis, stops the cell cycle in the G0/G1 phase, and increases mRNA expression levels of Trp53, Pak1, FAS, caspase-3, and caspase-9.[18]

In this study, a test using fluorescent Annexin V and HO/PI staining was carried out to determine whether the antitumor potential in vivo of complexes **1** and **2** is associated with the induction of death by apoptosis or necrosis. As shown in Figure 5(a), treatment of the mice with complexes **1** and **2** increased Annexin V positive cells, which suggests the induction of cellular death by apoptosis. Cell apoptosis is one of the main types of death and displays a range of common characteristics that involve a series of biochemical events and typical morphological changes.[49] The HO/PI double staining from EAC cells confirmed that complexes **1** and **2** caused cell death by apoptosis by changing the morphological features (Figure 5(c) and (d)). Chartterjee et al.[50] (also in vivo) examined the viability of cells post treatment with Ru(II)/arene/PTA complexes, called RAPTA-C, for Annexin V and PI double staining, by flow cytometry, and showed that treatment with the RAPTA-C in EAC-bearing mice induced apoptosis in EAC cells.

The apoptotic pathway is initiated by cleavage of caspase-3 and causes typical morphological changes including cell shrinkage, chromatin condensation, membrane blebbing, the appearance of membrane-associated apoptotic bodies, and DNA fragmentation.[49,51] Likewise, the morphological characteristics induced by complexes **1** and **2** (Figure 5(c)) were induced by caspase-3 activation (Figure 5(b)).

As shown in the cell cycle analysis (Figure 6), complexes **1** and **2** led to a significant increase in the EAC cells in the sub-G1 phase (fragmented DNA) when compared to the negative control, thereby leading to apoptosis. In addition, the percentage of cells in the G0/G1 phase also increased and was accompanied by a corresponding reduction in cells in the S and G2/M phases, thus stopping the progression of the cell cycle. Based on the principle that, among other typical features, apoptotic cells are characterized by DNA fragmentation and a consequent loss of nuclear DNA content, the treatment with complexes **1** and **2** led to EAC cell apoptosis due to increases in Annexin V positive cells and the percentage of cells in the sub-G1 phase.

CAM model has been widely used for monitoring tumor angiogenesis by inducing angiogenesis in several different types of tumor cells.[52–55] However, the induction of angiogenesis by EAC cells using CAM model was reported for the first time in this study. Complexes **1** and **2** reduced the angiogenic potential of EAC cells in CAM model (Figure 8), which is an interesting property for treatment of many cancers, especially for peritoneal carcinomatosis, because ascitic fluid is the direct nutritional source for tumor cells. It contains several growth factors and the nutrients needed for cell survival and proliferation. Rapid tumor growth leads to increased ascitic fluid perhaps to attend the high nutritional requirements of tumor cells.[24,39,56] Thereby, the results found indicate that the high antitumor potential of the complexes **1** and **2** in EAC-bearing mice led to increased MST and an increased life span, probably through the inhibition of angiogenesis induced by EAC cells and apoptosis induction of the EAC cells in vivo.

We demonstrated that the EAC cells treated with complexes **1** and **2** had reduction of glucose consumption

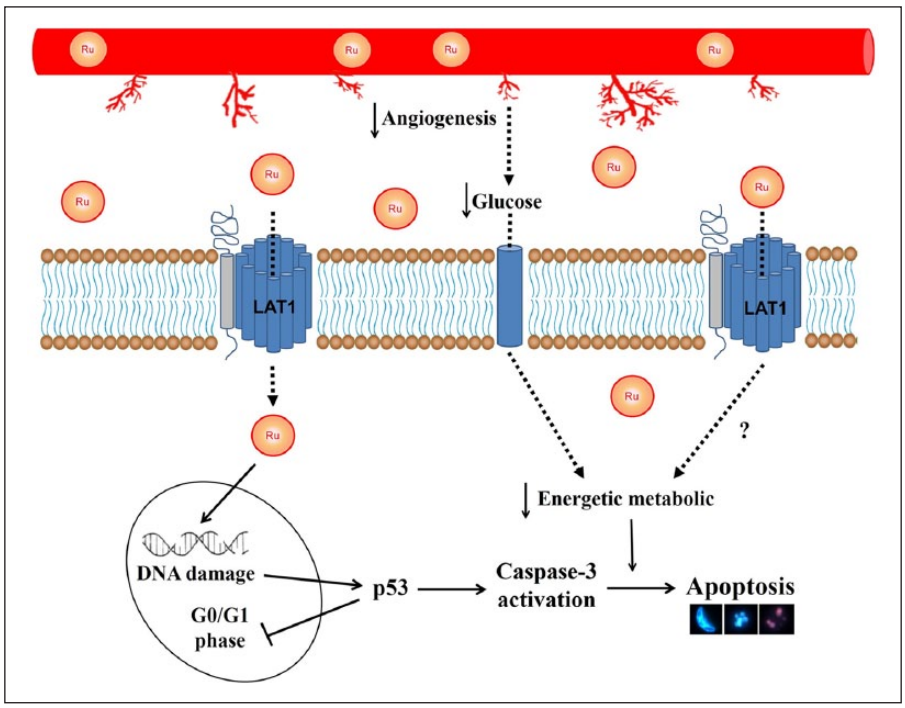

Figure 11. Hypothesis of effect of Ru(II)/amino acid/diphosphine complexes on tumor cells, suggesting that inhibition of angiogenesis reduces the glucose consumption in tumor cells and that LAT1 can be targeted by Ru(II)/amino acid/diphosphine complexes delivered into tumor cells, depriving supplementation of several growth factors and the nutrients needed for cell survival and proliferation, leading to apoptosis. Moreover, complexes **1** and **2** cause DNA fragmentation in vitro[18] and in vivo from EAC cells, increasing Trp53 expression,[18] G0/G1 phase cell cycle arrest, and finally cell death by caspase-3 mediated apoptosis.

(Figure 9), and this finding can be related with antiangiogenic potential. It has been reported that neoangiogenesis is necessary to provide glucose to cancer cells.[57] Furthermore, many cancer cells exhibit high glucose consumption aiming to increase cell proliferation and renewal.[58]

Likewise, cancer cells show reprogrammed energy metabolism, which results in a selective growth advantage and resistance to apoptotic death, since not only glucose but also other biomolecules, such as amino acids, are required for their survival and growth.[36,59,60]

The LAT1 are members of the sodium-independent amino acid transport system L, originally defined in the EAC cells, and are upregulated in human primary cancers and tumor cell lines, demonstrating an essential role for growth and survival.[61] Studies determining the function of LAT1 in cancer have used a well characterized LAT family inhibitor, BCH.[62] BCH is a model compound for the study of amino acid transporters, it is characterized as a system L competitive and selective inhibitor, particularly LAT1, capable of blocking the transport of amino acids into living cells and causing cell damage.[63] The inhibition of LAT1 activity has been proposed as oncology therapeutic implications, causing inhibition of cell growth and proliferation by deprivation of essential amino acids necessary for protein synthesis, cell growth, and proliferation.[64–67]

When LAT1 is blocked by BCH, it has been reported that the cell proliferation and DNA synthesis are suppressed,[33,62] apoptosis is induced in several types cancer cells,[67,68] and cleaved caspase-3 levels are increased.[63,68] As shown in Figure 10, EAC cells were sensitive to complexes **1** and **2**, and reduced the total cell number and ratio of cells (live/dead), but when they were previously treated with BCH, the same effect was not observed. The LAT1 could be associated with the mechanisms of growth inhibition of EAC cells in vitro and in vivo, allowing that Ru(II)/amino acid/diphosphine complexes could be (1) cytotoxic substrates that are delivered into the cell via LAT1, to act on an intracellular target and thereby promote tumor cell death or (2) inhibitors that selectively block transport by LAT1, and thereby deprive the tumor cells of the nutrients required for growth and proliferation. However, the relationship between LAT1 and the effect observed induced by complexes **1** and **2** in EAC cells is not clear. These results call for the undertaking of further studies to elucidate the mechanism by which Ru(II)/amino acid/diphosphine complexes interact with the LAT1 of tumor cells and cause tumor growth inhibition, apoptosis induction, and caspase-3 activation.

The inhibition of EAC cell angiogenesis probably reduces the supply of essential nutrients required, like glucose, for cell growth and survival leading to cell death by apoptosis. Likewise, our results show that these metal complexes could be cytotoxic substrates that are delivered into the cell via LAT1 or can block transport by LAT1 and

thereby promote tumor cell death. Our hypothesis for the inhibition of mechanisms of growth in EAC cells by complexes **1** and **2** is that the amino acids coordinated making these complexes more attractive, presenting antitumor potential by combination of different mechanisms of action inducing apoptosis with caspase activation and DNA damage (Figure 11).

Conclusion

In summary, the [Ru(L-Met)(bipy)(dppb)]PF_6 **(1)** and [Ru(L-Trp)(bipy)(dppb)]PF_6 **(2)** complexes demonstrated to be effective for peritoneal carcinomatosis treatment, and show high antitumor activity, with increased MST and ILS. Treatments with these complexes do not induce behavioral changes or signs of toxicity. These complexes are effective and safe, with fewer side effects than cisplatin. They induce apoptosis by combination of different mechanism of action, causing increased number of Annexin V positive cells, cleaved caspase-3, and of the sub-G1 peak in the cell cycle. In addition, the co-treatment of these complexes with EAC cells inhibited the angiogenesis in CAM model, leading to reduction of the glucose consumption post treatment. Moreover, it was observed that the sensitivity of EAC cells to the complexes decreases when the LAT1 is inhibited. The results of this study can support chronic study in vivo and clinical treatment.

Acknowledgements

The authors thank Julia Maria de Barros, Wildes Arantes de Moraes, and Vânia Beatriz Lopes Moura, PhD for technical assistance. The authors are grateful to Hugo Delleon da Silva, PhD for critically reading the manuscript.

Declaration of conflicting interests

The author(s) declared no potential conflicts of interest with respect to the research, authorship, and/or publication of this article.

Ethical approval

All procedures performed in the study involving animals were in accordance with the ethical standards of the institution or practice at which the studies were conducted. The procedures described were reviewed and approved by the Research Ethics Committee (CEUA) at the Federal University of Goiás (No. 039/2012).

Funding

The author(s) disclosed receipt of the following financial support for the research, authorship, and/or publication of this article: This study was financially supported by the Foundation for Research Support of the State of Goiás (FAPEG 2012/12), São Paulo Research Foundation (FAPESP 2014/10516-7), and the Coordination for the Improvement of Higher Education Personnel (CAPES 2014/1267732).

References

1. Su HT, Tsai CM and Perng RP. Peritoneal carcinomatosis in lung cancer. *Respirology* 2008; 13: 465–467.
2. Macrì A, Saladino E, Adamo V, et al. The treatment of peritoneal carcinomatosis in elderly patients. *BMC Geriatrics* 2010; 10: 1–2.
3. Zaslavsky A, Chen C, Grillo J, et al. Regional control of tumor growth. *Mol Cancer Res* 2010; 8: 1198–1206.
4. Hamilton CA, Maxwell GL, Chernofsky MR, et al. Intraperitoneal bevacizumab for the palliation of malignant ascites in refractory ovarian cancer. *Gynecol Oncol* 2008; 111: 530–532.
5. Sangisetty SL and Miner TJ. Malignant ascites: a review of prognostic factors, pathophysiology and therapeutic measures. *World J Gastrointest Surg* 2012; 4: 87–95.
6. Sano T. Is peritoneal carcinomatoses an incurable disease or controllable locoregional condition? Challenge of surgeons with intraperitoneal hyperthermic chemotherapy. *Jpn J Clin Oncol* 2001; 31: 1571–1572.
7. Sugarbaker PH. Overview of peritoneal carcinomatosis. *Cancerologia* 2008; 3: 119–124.
8. Ahmad S, Isab AA, Ali S, et al. Perspectives in bioinorganic chemistry of some metal based therapeutic agents. *Polyhedron* 2006; 25: 1633–1645.
9. Santos ER, Mondelli MA, Pozzi LV, et al. New ruthenium(II)/phosphines/diimines complexes: promising antitumor (human breast cancer) and Mycobacterium tuberculosis fighting agents. *Polyhedron* 2013; 51: 292–297.
10. Süss-Fink G. Arene ruthenium complexes as anticancer agents. *Dalton Trans* 2010; 39: 1673–1688.
11. Brabec V and Nováková O. DNA binding mode of ruthenium complexes and relationship to tumor cell toxicity. *Drug Resist Update* 2006; 9: 111–122.
12. Silveira-Lacerda EP, Vilanova-Costa CA, Pereira FC, et al. The ruthenium complex cis-(Dichloro)tetraammineruthenium(III) chloride presents immune stimulatory activity on human peripheral blood mononuclear cells. *Biol Trace Elem Res* 2010; 133: 270–283.
13. Bergamo A and Sava G. Ruthenium anticancer compounds: myths and realities of the emerging metal-based drugs. *Dalton Trans* 2011; 40: 7817–7823.
14. Heinrich TA, Poelhsits GV, Reis RI, et al. A new nitrosyl ruthenium complex: synthesis, chemical characterization, *in vitro* and *in vivo* antitumor activities and probable mechanism of action. *Eur J Med Chem* 2011; 46: 3616–3622.
15. Anchuri SS, Thota S, Yerra R, et al. Novel mononuclear ruthenium(II) compounds in cancer therapy. *Asian Pacific J Cancer Prev* 2012; 13: 3293–3298.
16. Lima AP, Pereira FC, Vilanova-Costa CA, et al. Induction of cell cycle arrest and apoptosis by ruthenium complex cis-(dichloro)tetramineruthenium(III) chloride in human lung carcinoma cells A549. *Biol Trace Elem Res* 2012; 147: 8–15.
17. Lima AP, Pereira FC, Almeida MA, et al. Cytoxicity and apoptotic mechanism of ruthenium(II) amino acid complexes in sarcoma-180 tumor cells. *PLoS ONE* 2014; 9: e10865.
18. Porto HKP, Vilanova-Costa CAST, Mello FMS, et al. Synthesis of a ruthenium(II) tryptophan-associated complex and biological evaluation against Ehrlich murine breast carcinoma. *Transition Met Chem* 2014; 40: 1–10.

19. Wu Q, He J, Mei W, et al. Arene ruthenium(II) complex, a potent inhibitor against proliferation, migration and invasion of breast cancer cells, reduces stress fibers, focal adhesions and invadopodia. *Metallomics* 2014; 6: 2204–2212.
20. Almeida MAP, Nascimento FB, Graminha AE, et al. Structural features and cytotoxic activities of [Ru(AA-H)(dppb)(bipy)] PF6 complexes. *Polyhedron* 2014; 81: 735–742.
21. Ehrlich P and Apolant H. Zur Kenntnis der Sarkomentwicklung bei Carcinomtransplantationen. *Zentralbl Allg Pathol* 1906; 17: 513–515.
22. Ozaslan M, Karagoz ID, Kilic IH, et al. Ehrlich ascites carcinoma. *Afr J Biotechnol* 2011; 10: 2375–2378.
23. Calixto-Campos C, Zarpelon AC, Corrêa M, et al. The Ehrlich tumor induces pain-like behavior in mice: a novel model of cancer pain for pathophysiological studies and pharmacological screening. *BioMed Res Int* 2013; 2013: 624815.
24. Menezes CSR, Costa LCGP, Ávila VMR, et al. Analysis *in vivo* of antitumor activity, Citotoxicity and Interaction between plasmid DNA and the *cis*-dichlorotetramineruthenium (III) chloride. *Chem Biol Interact* 2007; 167: 116–124.
25. Kviecinski MR, Benelli P, Felipe KB, et al. SFE from Bidens pilosa Linné to obtain extracts rich in cytotoxic polyacetylenes with antitumor activity. *J Supercrit Fluids* 2011; 56: 243–248.
26. Sunil D, Isloor AM, Shetty P, et al. *In vivo* anticancer and histopathology studies of Schiff bases on Ehrlich ascitic carcinoma cells. *Arabian J Chem* 2013; 6: 25–33.
27. Malone MH and Robichaud RD. A hippocratic screen for pure or crude drug materials. *Lloydia* 1962; 25: 320–332, http://www.fcfar.unesp.br/arquivos/483524.pdf
28. Syed Abdul Rahman SN, Abdul Wahab N and Abd Malek SN. In vitro morphological assessment of apoptosis induced by antiproliferative constituents from the rhizomes of Curcuma zedoaria. *Evid Based Complement Alternat Med* 2013; 2013: 257108.
29. Rogalska A, Marczak A, Gajek A, et al. Induction of apoptosis in human ovarian cancer cells by new anticancer compounds, epothilone A and B. *Toxicol In Vitro* 2013; 27: 239–249.
30. Sathisha MP, Revankar VK and Pai KSR. Synthesis, structure, electrochemistry, and spectral characterization of bis-isatin thiocarbohydrazone metal complexes and their antitumor activity against Ehrlich ascites carcinoma in Swiss albino mice. *Met Based Drugs* 2008; 2008: 362105.
31. Melo-Reis PR, Andrade LS, Silva CB, et al. Angiogenic activity of Synadenium umbellatum Pax latex. *Braz J Biol* 2010; 70: 189–194.
32. Fu YM, Lin H, Liu X, et al. Cell death of prostate cancer cells by specific amino acid restriction depends on alterations of glucose metabolism. *J Cell Physiol* 2010; 224: 491–500.
33. Lin J, Raoof DA, Thomas DG, et al. L-type amino acid transporter-1 overexpression and melphalan sensitivity in Barrett's adenocarcinoma. *Neoplasia* 2004; 6: 74–84.
34. Castello Branco ACS, Diniz MFF, Almeida RN, et al. Parâmetros bioquímicos e hematológicos de ratos Wistar e camundongos Swiss do Biotério Professor Thomas George. *Rev Bras Ciên Saúde* 2011; 15: 209–214.
35. Nishida N, Yano H, Nishida T, et al. Angiogenesis in cancer. *Vasc Health Risk Manag* 2006; 2: 213–219.
36. Hananhan D and Weinberg RA. Hallmarks of cancer: the next generation. *Cell* 2011; 144: 646–674.
37. Lokman NA, Elder ASF, Ricciardelli C, et al. Chick chorioallantoic membrane (CAM) assay as an *in vivo* model to study the effect of newly identified molecules on ovarian cancer invasion and metastasis. *Int J Mol Sci* 2012; 13: 9959–9970.
38. Zhao Y, Wang L and Pan J. The role of L-type amino acid transporter 1 in human tumors. *Intractable Rare Dis Res* 2015; 4: 165–169.
39. Dolai N, Karmakar I, Suersh Kumar RB, et al. Evaluation of antitumor activity and in vivo antioxidant status of Anthocephalus cadamba on Ehrlich ascites carcinoma treated mice. *J Ethnopharmacol* 2012; 142: 865–870.
40. Araújo JGC, Mota LG, Leite EA, et al. Biodistribution and antitumoral in Ehrlich tumor-bearing mice. *Exp Biol Med* 2011; 236: 808–815.
41. Maroni LC, Silveira ACO, Leite EA, et al. Antitumor effectiveness and toxicity of cisplatin-loaded log-circulating and pH-sensitive liposomes against Ehrlich ascitic tumor. *Exp Biol Med* 2012; 237: 973–984.
42. Haldar PK, Kar B, Bala A, et al. Antitumor activity of Sansevieria roxburghiana rhizome against Ehrlich ascites carcinoma in mice. *Pharm Biol* 2010; 48: 1337–1343.
43. Lokich J and Anderson N. Carboplatin versus cisplatin in solid tumors: analysis of the literature. *Ann Oncol* 1998; 9: 13–21.
44. Keppler BK, Berger MR and Heim ME. New tumor-inhibiting metal complexes. *Cancer Treatment Rev* 1990; 17: 261–277.
45. Zeng L, Chen Y, Liu J, et al. Ruthenium(II) complexes with 2-phenylimidazo[4,5-f][1,10]phenanthroline derivatives that strongly combat cisplatin-resistant tumor cells. *Sci Rep* 2016; 6: 19449.
46. Puckett CA and Barton JK. Methods to explore cellular uptake of ruthenium complexes. *J Am Chem Soc* 2007; 129: 46–47.
47. Liu Z, Habtemariam A, Pizarro AM, et al. Organometallic iridium(III) cyclopentadienyl anticancer complexes containing C,N-chelating ligands. *Organometallics* 2011; 30: 4702–4710.
48. McKeage M, Berners-Price S, Galettis P, et al. Role of lipophilicity in determining cellular uptake and antitumour activity of gold phosphine complexes. *Cancer Chemother Pharmacol* 2000; 46: 343–350.
49. Galluzzi L, Vitale I, Abrams JM, et al. Molecular definitions of cell death subroutines: recommendations of the nomenclature committee on cell death. *Cell Death Differ* 2012; 19: 107–120.
50. Chartterjee S, Kundu S, Bhattacharyya A, et al. The ruthenium(II)-arene compound RAPTA-C induces apoptosis in EAC cells through mitochondrial and p53-JNK pathways. *J Biol Inorg Chem* 2008; 7: 1149–1155.
51. Elmore S. Apoptosis: a review of programmed cell death. *Toxicol Pathol* 2007; 35: 495–516.
52. Richardson M, Elmore S and Sigh G. Observations on the use of the avian choriallantoic membrane (CAM) model in investigations into angiogenesis. *Curr Drug Targets Cardiovasc Hematol Disord* 2003; 3: 155–185.
53. Manjunathan R and Ragunathan M. Chicken chorioallantoic membrane as a reliable model to evaluate osteosarcoma—an experimental approach using SaOS2 cell line. *Biol Proced Online* 2015; 17: 10.

54. Busch C, Krochmann J and Drews U. The chick embryo as an experimental system for melanoma cell invasion. *PLoS ONE* 2013; 8: e53970.
55. Liu M, Scanlon CS, Banerjee R, et al. Choriollantoic membrane assay: vascularized 3-dimensional cell culture system for human prostate cancer cells as an animal substitute model. *J Urol* 2001; 166: 1502–1507.
56. Prasad SB and Giri A. Antitumor effect of cisplatin against murine ascites Dalton's lymphoma. *Indian J Exp Biol* 1994; 32: 155–162.
57. de Laplanche E, Boudria A, Dacheux E, et al. Low glucose microenvironment of normal kidney cells stabilizes a subset of messengers involved in angiogenesis. *Physiol Rep* 2015; 3: e12253.
58. Locasale JW and Cantley LC. Metabolic flux and the regulation of mammalian cell growth. *Cell Metab* 2011; 14: 443–451.
59. Dang CV. Links between metabolism and cancer. *Genes Dev* 2012; 26: 877–890.
60. Jang M, Kim SS and Lee J. Cancer cell metabolism: implications for therapeutic targets. *Exp Mol Med* 2013; 45: e45.
61. Barker GA and Ellory JC. The identification of neutral amino acid transport systems. *Exp Physiol* 1990; 75: 3–26.
62. Wang Q and Holst J. L-type amino acid transport and cancer: targeting the mTORC1 pathway to inhibit neoplasia. *Am J Caner Res* 2015; 5: 1281–1294.
63. Kim CS, Moon IS, Park JH, et al. Inhibition of L-type amino acid transporter modulates the expression of cell cycle regulatory factors in KB oral cancer cells. *Biol Pharm Bull* 2010; 33: 1117–1121.
64. Ohkame H, Masuda H, Ishii Y, et al. Expression of L-type amino acid transporter 1 (LAT1) and 4F2 heavy chain (4F2hc) in liver tumor lesions of rat models. *J Surg Oncol* 2001; 78: 265–271.
65. Kim DK, Kanai Y, Choi HW, et al. Characterization of the system L amino acid transporter in T24 human bladder carcinoma cells. *Biochim Biophys Acta* 2002; 1565: 112–121.
66. Fuchs BC and Bode BP. Amino acid transporters ASCT2 and LAT1 in cancer: partners in crime? *Semin Cancer Biol* 2005; 15: 254–266.
67. Kim CS, Cho SH, Chun HS, et al. BCH, an inhibitor of system L amino acid transporters, induces apoptosis in cancer cells. *Biol Pharm Bull* 2008; 31: 1096–1100.
68. Kobayashi K, Ohnishi A, Promsuk J, et al. Enhanced tumor growth elicited by L-type amino acid transporter 1 in human malignant glioma cells. *Neurosurgery* 2008; 62: 493–503.